A Loop between Transmembrane Helices IX and X of Subunit I of Cytochrome *c* Oxidase Caps the Heme *a*–Heme a_3–Cu_B Center†

Jonathan P. Hosler,‡ James P. Shapleigh,§,∥ Mary M. J. Tecklenburg,⊥,# Jeffrey W. Thomas,§ Younkyoo Kim,⊥,▽ Matthew Espe,⊥ John Fetter,‡ Gerald T. Babcock,⊥ James O. Alben,○ Robert B. Gennis,§ and Shelagh Ferguson-Miller*,‡

Departments of Biochemistry and Chemistry, Michigan State University, East Lansing, Michigan 48824, Department of Biochemistry, University of Illinois, Urbana, Illinois 61801, and Department of Medical Biochemistry, Ohio State University, Columbus, Ohio 43210

Received August 6, 1993; Revised Manuscript Received November 15, 1993⊛

ABSTRACT: Site-directed mutants were prepared of four consecutive and highly conserved residues (His-411, Asp-412, Thr-413, Tyr-414) of an extramembrane loop that connects putative transmembrane helices IX and X of subunit I of *Rhodobacter sphaeroides* cytochrome *c* oxidase. The modified enzymes were purified and analyzed by optical, resonance Raman, FTIR, and EPR spectroscopies. Consistent with our recent model in which both hemes are ligated to histidines of helix X [Hosler, J. P., et al. (1993) *J. Bioenerg. Biomembr. 25*, 121–136], substitutions for three of these four residues cause perturbations of either heme *a* or heme a_3. Resonance Raman spectra of the mutant Y414F demonstrate that Tyr-414 does not participate in a hydrogen bond with the heme *a* formyl group, but its alteration does result in a 5-nm red-shift of the α-band of the visible spectrum, indicating proximity to heme *a*. The mutant D412N shows changes in resonance Raman and FTIR difference spectra indicative of an effect on the proximal ligation of heme a_3. Changing His-411 to alanine has relatively minor effects on the spectral and functional properties of the oxidase; however, FTIR spectra reveal alterations in the environment of Cu_B. Conversion of this residue to asparagine strongly disrupts the environment of heme a_3 and Cu_B and inactivates the enzyme. These results suggest that His-411 is very near the heme a_3–Cu_B pocket. We propose that these residues form part of a cap over the heme *a*–heme a_3–Cu_B center and thus are important in the structure of the active site.

Bacterial homologues of the complex eukaryotic cytochrome *c* oxidases provide convenient model systems for investigation of structure–function relationships by site-directed mutagenesis (Hosler et al., 1993; Shapleigh et al., 1992a; Lemieux et al., 1992; Minagawa et al., 1992). Although there is no crystal structure to aid in the design and interpretation of mutational studies, the analysis of mutant forms is facilitated by the wealth of spectroscopic data available for the mammalian cytochrome aa_3. Indeed, the UV–visible, IR,[1] resonance Raman, and EPR spectra of cytochrome aa_3 of *Rhodobacter sphaeroides* are remarkably similar to those of beef heart cytochrome oxidase (Hosler et al., 1992; Shapleigh et al., 1992a), as would be predicted from the high degree of amino acid sequence homology (Cao et al., 1991, 1992; Shapleigh & Gennis, 1992). Interpretation of the spectral features of the bacterial oxidase can thus be made directly on the basis of knowledge gained for the mammalian enzyme. Conversely, the ability to specifically modify the structure of the bacterial enzyme provides a means of further deciphering the factors that determine the spectroscopic characteristics of the native oxidases.

In this regard, an interesting spectroscopic feature of bacterial and mammalian oxidases is the red-shift (from 595 to 605 nm) of the α-band of heme *a* compared to heme A:*bis*-imidazole models of this low-spin center (Babcock et al., 1979; Callahan & Babcock, 1983; Babcock, 1988). This appears to result from a strong hydrogen bond between the formyl group on the heme *a* porphyrin ring and a proton donor in the protein (Callahan & Babcock, 1983). A highly conserved tyrosine, corresponding to residue 414 in *Rb. sphaeroides* subunit I, has been implicated in this interaction (Saraste, 1990). Hydropathy plot analysis of subunit I places Tyr-414 in an extramembrane segment between transmembrane helices IX and X [see Figure 1 in Hosler et al. (1993)]. This loop contains three other highly conserved residues His-411, Asp-412, and Thr-413, adjacent to Tyr-414. Each of these is capable of hydrogen bonding. His-411 has also been suggested to ligate heme *a* (Saraste, 1990). However, current evidence rules out this latter role, since the results of site-directed mutagenesis strongly implicate His-421 in helix X, along with His-102 in helix II, as the actual ligands of heme *a* (Shapleigh et al., 1992a; Hosler et al., 1993).

According to the current working model derived from analysis of site-directed mutants (Hosler et al., 1993), Tyr-414 (or adjacent residues) could still participate in a hydrogen

† This work was supported by National Institutes of Health Grants GM26916 (to S.F.-M.), GM37300 and GM25480 (to G.T.B., supporting M.E. and Y.K.), HL16101 (to R.B.G.), GM 13047 (to M.M.J.T.), and HL07404, a Cardiovascular Training Grant (supporting J.F.), by the Research Excellence Fund, State of Michigan, and the All University Research Initiation Grant, MSU (to J.P.H. and S.F.-M.), by the National Science Foundation (DMB89-04614 to J.O.A.), and by the Human Frontier Science Program (to R.B.G.).

‡ Department of Biochemistry, Michigan State University.

§ Department of Biochemistry, University of Illinois, Urbana.

∥ Present address: Department of Microbiology, Cornell University, Ithaca, NY.

⊥ Department of Chemistry, Michigan State University.

Present address: Department of Chemistry, Central Michigan University, Mt. Pleasant, MI.

▽ Present address: Department of Chemistry, Hankuk University of Foreign Studies, Yongin-gun, Kyungki-do 449-791, Korea.

○ Department of Medical Biochemistry, Ohio State University.

⊛ Abstract published in *Advance ACS Abstracts,* January 15, 1994.

[1] Abbreviations: RR, resonance Raman; EPR, electron paramagnetic resonance; IR, infrared; FTIR, Fourier transform infrared.

0006-2960/94/0433-1194$04.50/0

Table 1: Absorbance Maxima, Heme *a* and a_3 Content, CO Binding, and Electron Transfer Activities of the Wild-Type and Mutant Oxidases

oxidase	α_{max} (nm)	$Soret_{max}$ (nm)	$Soret_{max}/\alpha_{max}$	% CO binding (compared to wild-type)	CO difference spectrum minimum	% contamination by hemes C + B[a]	heme a_3 content per cytochrome aa_3 monomer	electron transfer activity (% of wild-type)[b]
wild-type	605.4	444.4	5.3	(100)	446.7	7	normal (100%)	(100)
Y414F	610.0	445.6	5.2	100	446.7	7	normal	69
T413N	605.4	443.8	5.4	91	446.7	7	normal	94
D412N	605.4	443.8	5.2	90	446.7	10	normal	44
H411A	604.8	443.8	5.3	84	446.7	4	normal	50
H411N	604.2	441.1[c]	4.0[c]	16	443.8	44	~40%	0

[a] Based upon pyridine hemochrome spectra. [b] From a representative polarographic experiment, performed as in Hosler et al. (1992), but using 38 μM horse heart cytochrome *c*. The turnover number of the wild-type enzyme was 1523 s^{-1}. [c] These values include some artifact due to contaminating *b* and *c* cytochromes in the preparation of the H411N mutant (Figure 3 and text).

bond with the heme *a* formyl group. To test this postulate, Tyr-414 was converted to phenylalanine, and the other three conserved residues were also modified: His-411 to asparagine and alanine, Asp-412 to asparagine, and Thr-413 to asparagine. The results demonstrate that the alteration of three of these residues differentially influences the spectroscopic properties of heme *a* and the heme a_3–Cu_B center, suggesting that this region of the loop spans the distance between heme *a* and heme a_3, consistent with models in which both hemes are bound to helix X (Hosler et al., 1993; Brown et al., 1993; Calhoun et al., 1993). However, none of these residues appear directly involved in a hydrogen bond with the heme *a* formyl group.

EXPERIMENTAL PROCEDURES

All materials were prepared or purchased as in Hosler et al. (1992). Site-directed mutagenesis and isolation of the mutant *Rb. sphaeroides* strains was performed as described in Shapleigh et al. (1992a). *Rb. sphaeroides* CY91, obtained from C. Yun (of the Gennis group at the University of Illinois), was used as the wild-type strain for the biochemical and spectral analyses. Bacterial growth, oxidase purification, electron transfer activity measurements, and optical, resonance Raman (RR), and electron paramagnetic resonance (EPR) spectroscopy were performed as described in Hosler et al. (1992), with the exceptions noted in the figures legends and in Table 1. Low-temperature Fourier transform infrared (FTIR) difference spectra were obtained as described in Shapleigh et al. (1992b).

Pyridine Hemochromagen Analysis of Heme A, B, and C. Dithionite-reduced *minus* ferricyanide oxidized spectra were obtained for the oxidase samples, after adding pyridine to a final concentration of 10% (vol/vol) and NaOH to 0.2 N. The concentrations of hemes A, B, and C were obtained by the calculations of Berry and Trumpower (1987).

Estimation of the Heme a_3 Content. The heme A concentration was compared to the concentration of cytochrome aa_3, determined from the α-band absorbance (ϵ = 40 cm^{-1} mM^{-1}) of absolute reduced spectra of the oxidases. For the wild-type enzyme, the concentration of heme A is twice that of the concentration of cytochrome aa_3, indicating normal amounts of both hemes *a* and a_3. The loss of heme a_3 (in H411N only; see below) is indicated by a heme A concentration that is less than twice the calculated concentration of cytochrome aa_3. The loss can be assigned to heme a_3 based on the Soret to α-band ratio (see below).

Determination of the Extent of CO Binding. The reduced cytochrome aa_3–CO adduct was obtained by slow bubbling of 1 mL of CO through a sample of dithionite-reduced oxidase. This procedure gives full CO binding in the wild-type enzyme (Hosler et al., 1992). The extent of CO binding to the mutant oxidases, relative to wild-type, was determined by comparing the ratio of the magnitude of the absorbance minimum of the CO difference spectra (480 nm *minus* 446.7 nm) and the magnitude of the α-band of the fully reduced enzyme (605 nm *minus* 650 nm). For the wild-type oxidase the ratio of these absorbance changes equals 2.0. Hence, this method gives values that represent CO bound per unit heme *a*. Alternatively, the absolute concentration of heme a_3–CO was determined using $\Delta\epsilon_{590nm\ minus\ 612nm}$ of 9.9 cm^{-1} mM^{-1} for the reduced-CO *minus* reduced spectra (Vanneste, 1966). Both methods gave the same estimate of percent CO binding.

RESULTS

The effect of substitutions at all four residues is summarized in Table 1. Four of the five mutants were stable to purification and could be obtained in a highly purified state with no apparent change in spectral characteristics compared to the membrane-bound form. Although this was true when His-411 was converted to alanine, substitution of asparagine at this position resulted in a less stable protein that was difficult to purify and appeared to lose a significant amount of heme a_3 in the process. In EPR studies (to be presented elsewhere) all five mutants showed a normal Cu_A and maintained a spin-coupled heme a_3–Cu_B center, as indicated by lack of an appreciable high spin heme a_3 signal at g = 6.0. With the exception of H411N, all the mutants showed relatively small changes in spectral properties compared to wild-type, and all retained significant activity. The analysis of individual mutant forms by resonance Raman, FTIR, and UV–visible spectroscopy is detailed below.

Histidine 411. This residue was substituted by both alanine and asparagine. The fact that H411A retains activity (Table 1) and a wild-type resonance Raman spectrum [see Shapleigh et al. (1992a)] has already been used to argue that this histidine is not a redox center ligand (Shapleigh et al., 1992a; Hosler et al., 1993). However, the α and Soret peaks of H411A are slightly blue-shifted (Figure 3; Table 1), indicating some alteration of the heme environments. Furthermore, while the peak position of the CO difference spectrum is identical to that of the wild-type enzyme (Figure 4; Table 1), the extent of CO binding to heme a_3 is slightly reduced to 84% of the wild-type level.

The substitution of asparagine at position 411 introduces a residue with a partial specific volume (Zamyatnin, 1972) and hydropathy value (Kyte & Doolittle, 1982) similar to those of histidine. However, the results of this alteration are much more detrimental than replacement of His-411 by alanine. An inactive oxidase is obtained (Table 1) with many characteristics similar to mutants of the histidines that ligate the heme a_3–Cu_B center (Shapleigh et al., 1992a). This mutant oxidase was difficult to purify due to instability; the preparation used for analysis was still substantially contaminated with *b* and *c* cytochromes, by pyridine hemochrome analysis (Table

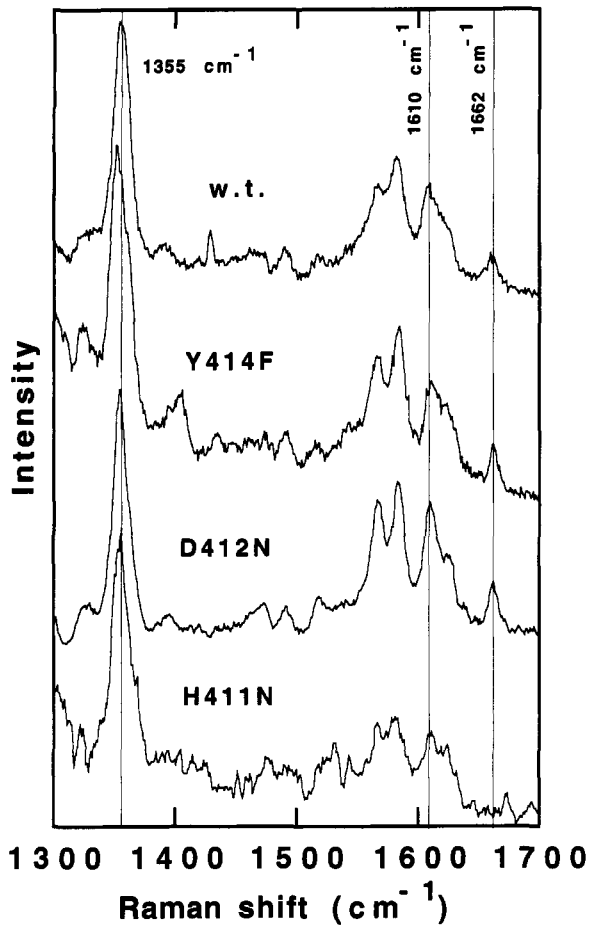

FIGURE 1: Resonance Raman spectra of the high-frequency region of purified, dithionite-reduced wild-type cytochrome *c* oxidase and oxidases containing mutations in the IX–X loop. The formyl stretching modes of heme *a* (1610 cm^{-1}) and heme a_3 (1662 cm^{-1}) are marked. The electron-density marker at 1355 cm^{-1} (ν_4) is at the wild-type frequency for all of the mutants, within the error of the spectrometer resolution. The spectra of T413N and H411A are identical to that of wild-type and have been omitted. The exciting laser wavelength was 441.6 nm.

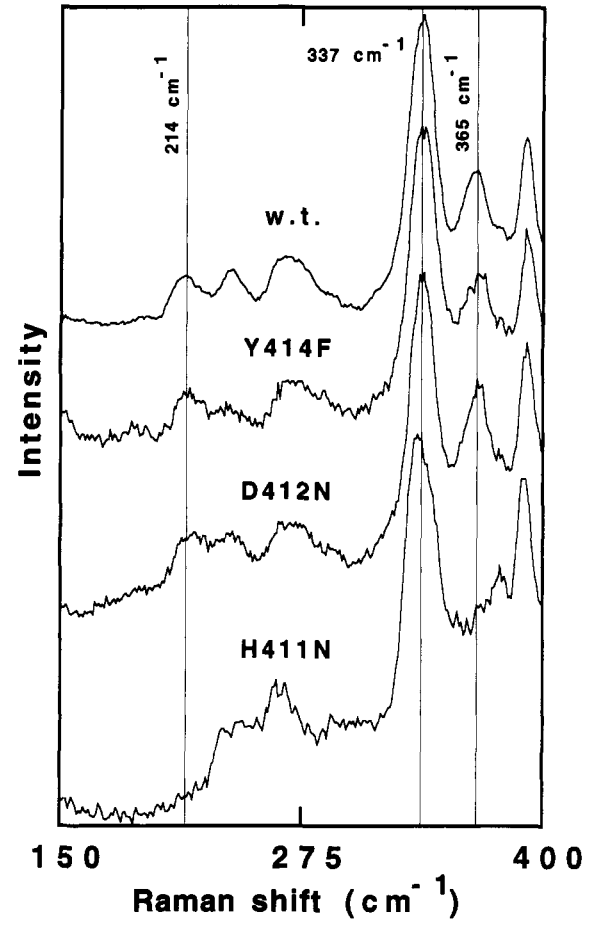

FIGURE 2: Resonance Raman spectra of the low frequency region of wild-type and the loop mutants. The Fe–N_{His} stretch (214 cm^{-1}) and the ring bending mode (365 cm^{-1}) of heme a_3 are marked. The spectra of T413N and H411A are identical to that of wild-type and have been omitted. The exciting laser wavelength was 441.6 nm.

1). In spite of this contamination, a 1.2-nm blue-shift is clearly visible in the α-band of the purified enzyme and is also seen in the membrane-bound form. The Soret band appears to be blue-shifted by 3 nm, but this is an inaccurate estimate due to contamination by *b* and *c* cytochromes. The true shift can be estimated at ~2.3 nm. The majority of the Soret shift is likely due to heme a_3, since the CO difference spectrum (Figure 4) shows a shift in the 446.7 nm minimum to 443.8 nm and an overall reduction in CO binding to only 16% of the level observed with the wild-type oxidase (Table 1).

Comparison of absolute reduced and pyridine hemochrome spectra (see Experimental Procedures) indicates that 30% of the normal amount of heme A is lost in purified H411N. Since the optical and RR spectra (Figures 1–3) show little change in the heme *a* environment, loss of the low-spin heme is unlikely. It is assumed that all of the heme A is lost from the highly disturbed heme a_3 site, leading to an estimated heme a_3 content of ~40%. The low Soret/α value of purified H411N (Table 1) is another indicator of the loss of heme a_3, since only loss of the high-spin heme could lead to a decrease in this ratio [see Vanneste (1966)].

At early stages in the preparation of H411N, the level of CO binding to heme a_3 is observed to be ~35% of the wild-type level, compared to ~16% in more highly purified preparations. This suggests that much of the loss of heme a_3 in H411N occurs during purification, presumably because of the protein instability discussed above.

Resonance Raman (RR) spectroscopy is particularly useful in the interpretation of structural changes introduced by mutation because of its ability to distinguish vibrational modes that arise specifically from either heme *a* or a_3. These modes reflect the interactions of each heme with its immediate protein environment (Babcock, 1988; Ching et al., 1985). The similarity of the spectra of mammalian and *Rb. sphaeroides* cytochrome aa_3 has already been documented (Hosler et al., 1992; Shapleigh et al., 1992a). In the RR spectrum of H411N, but not H411A, three modes specific to heme a_3, the Fe–N_{His} stretch at 214 cm^{-1}, the ring bending mode at 365 cm^{-1}, and the formyl stretch at 1662 cm^{-1}, are absent (Figures 1 and 2). Since approximately 60% of purified H411N lacks heme a_3, significant loss of the heme a_3 modes would be expected. The loss of these modes in the remaining population likely results from excessive broadening of the peaks, as a distorted binuclear pocket may allow multiple orientations of the heme and its substituent groups. (The weak band seen at 1675 rather than 1662 cm^{-1} may arise from the heme a_3 formyl group if it is less conjugated with the heme π system.) Two modes specific for heme *a*, the vinyl and formyl stretches at 1611 and 1625 cm^{-1}, respectively, are unaltered in both H411A and H411N, demonstrating that the protein environment of heme *a* is similar to that of the wild-type enzyme, including the proposed hydrogen bond to the heme *a* formyl (Callahan & Babcock, 1983).

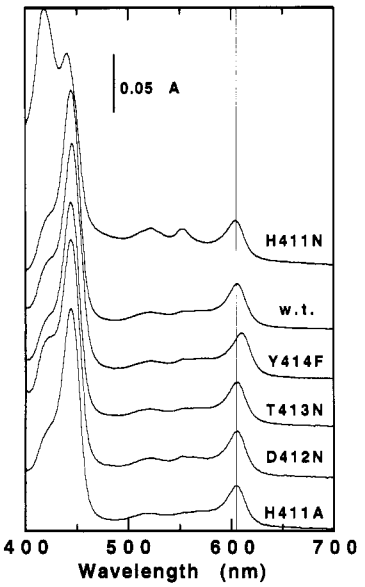

FIGURE 3: Absolute optical spectra of purified, dithionite-reduced wild-type cytochrome *c* oxidase and oxidases containing mutations in the IX–X loop of subunit I. The spectra are normalized to each other to account for concentration differences. The marking line is placed at 605.4 nm. All of these enzymes were purified as in Hosler et al. (1992). The spectrum of H411N shows that this mutant is particularly difficult to separate from other membrane-bound cytochrome complexes, most likely because of its slightly unstable structure as discussed in the text.

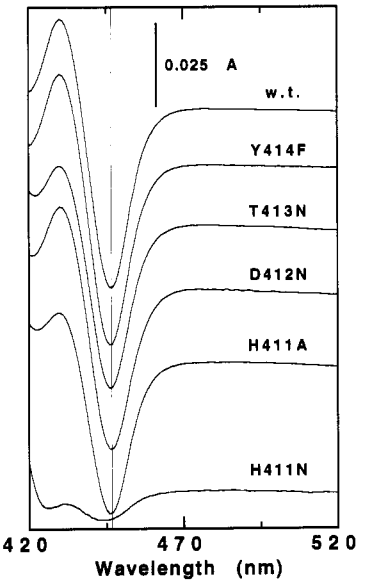

FIGURE 4: Carbon monoxide difference spectra (CO-bound, dithionite-reduced *minus* reduced) of wild-type oxidase and the loop mutants. The trough of the wild-type difference spectrum at 446.7 nm is marked for reference.

The C≡O stretching frequencies of both H411A and H411N, in their membrane-bound form, were analyzed by Fourier transform infrared difference spectroscopy (FTIR) at low temperature. This technique is a sensitive probe of the local molecular environment of the oxygen binding pocket, since at low temperature CO can be photolyzed from heme a_3 and bound to Cu_B (Fiamingo et al., 1982). Spectra of the wild-type oxidase exhibit two Fe–C≡O maxima, one at 1950 cm^{-1} and the other at 1964 cm^{-1}, and two Cu–C≡O maxima at 2039 and 2060 cm^{-1} (Shapleigh et al., 1992b). The CO adduct of H411A gives a spectrum very similar to that of the native enzyme [Figure 5; compare to Shapleigh et al. (1992b)], including the distinctive narrow bandwidth of the Fe–C≡O

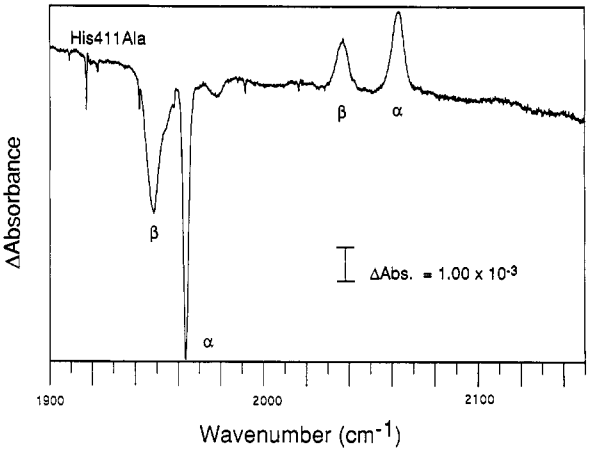

FIGURE 5: Low temperature (10 K) FTIR difference spectrum (light *minus* dark) of membrane-bound, CO-ligated H411A. Conditions are as described in Shapleigh et al. (1992b). The α and β forms of the C≡O(Fe) and C≡O(Cu) signals are labeled. The α Fe–C≡O signal appears at 1964 cm^{-1}, as in the spectrum of the wild-type enzyme, while the α Cu–C≡O signal is shifted up by 4 cm^{-1}, to 2064 cm^{-1}.

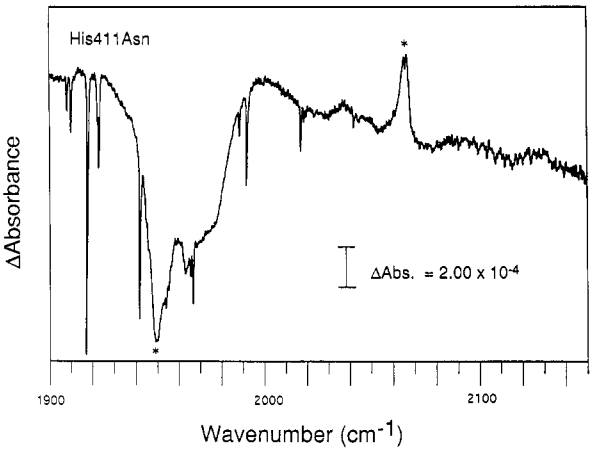

FIGURE 6: Low temperature FTIR difference spectrum of membrane-bound, CO-ligated H411N. Conditions are as in Figure 5. The starred (*) signals are the Fe–C≡O and Cu–C≡O stretches arising from the *cb*-type oxidase that predominates in cells containing an inactive aa_3-type oxidase [see Shapleigh et al. (1992b)].

signal (Alben & Fiamingo, 1984; Yoshikawa & Caughey, 1982) appearing at 1964 cm^{-1}. However, the Cu–C≡O signals are altered, showing a shift of 4 cm^{-1} in the α form (to 2064 cm^{-1}) and a narrowing of the β form (Figure 5), indicating some change in the Cu_B–C≡O environment in this active oxidase mutant.

The FTIR difference spectrum of H411N (Figure 6) shows a highly distorted a_3–Cu_B center, consistent with the loss of enzymatic activity, loss of much of the heme a_3 (Table 1), and a perturbed RR spectrum (Figures 1 and 2). The CO that binds to the remaining heme a_3 appears to be in a more disordered, polar binuclear center pocket, as indicated by the broad Fe–C≡O peak extending from 1960 to 1980 cm^{-1} and no detectable Cu_B–C≡O signal. [The Cu–C≡O at 2065 cm^{-1} and the Fe–C≡O at 1950 cm^{-1} in the spectrum of H411N are due to the *cb*-type cytochrome *c* oxidase that predominates in *Rb. sphaeroides* cells lacking an active aa_3-type oxidase (Shapleigh et al., 1992b)]. Despite the lack of the Cu_B–C≡O signal in the FTIR difference spectrum of H411N membranes, EPR experiments (discussed above) suggest that Cu_B is still physically present in the ~40% of purified H411N that retains heme a_3.

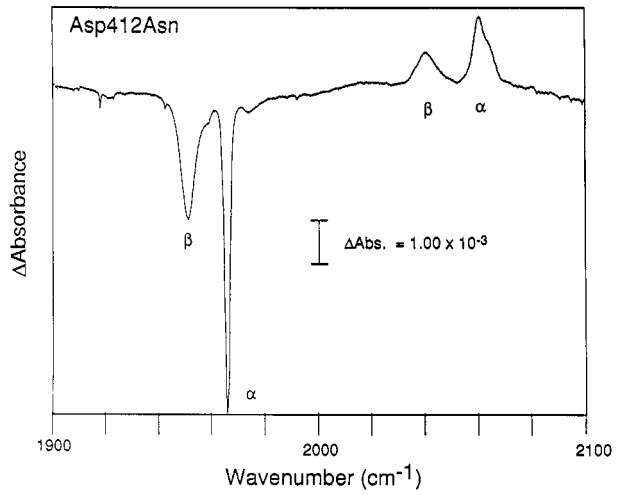

FIGURE 7: Low temperature FTIR difference spectrum of membrane-bound, CO-ligated D412N. Conditions and labels are as in Figure 5. The α Fe–C≡O signal appears at 1966 cm^{-1}, rather than at 1964 cm^{-1} as wild-type. All of the other signals are unchanged from wild-type.

Aspartate 412. Alteration of this residue to its amide form leads to ~50% loss in electron transfer activity (Table 1), but spectral analysis indicates no major structural change. The optical spectrum shows a slight blue-shift (~0.5 nm) of the Soret band (Figure 3; Table 1), but no shift of the α-band, similar to T413N (see below). The CO difference spectrum is wild-type (Figure 4), although a small reduction in the extent of CO binding (10%) is evident (Table 1). The RR spectrum of D412N (Figures 1 and 2) is unchanged from that of wild-type in all respects but one: a shift of the $Fe-N_{His}$ stretch of heme a_3 from 214 to 218 cm^{-1} indicates a slight strengthening of this bond. The FTIR spectrum of D412N (Figure 7) is also similar to that of wild-type (Shapleigh et al., 1992b), except for a 2-cm^{-1} shift in the Fe–C≡O signal (from 1964 to 1966 cm^{-1}).

Threonine 413. The T413N mutant is the least altered of the mutants presented here. Apart from a <10% loss in electron transfer activity (Table 1), a 0.5-nm blue-shift of the Soret band (Figure 3; Table 1), and a <10% reduction in the level of CO binding (Table 1), all of the other spectral characteristics, including the CO difference (Figure 4), RR, EPR, and FTIR spectra (not shown), are identical to those of the wild-type oxidase.

Tyrosine 414. The conversion of Tyr-414 to phenylalanine results in ~30% loss in activity, but with no apparent perturbation of heme *a* or heme a_3, as measured by RR spectroscopy (Figures 1 and 2). In contrast, the optical α-band of purified (or membrane-bound) Y414F (Figure 3) is red-shifted by 4.5 nm (Table 1), clearly showing that the absorbance of heme *a* has been altered. Since the CO difference spectrum (Figure 4) is unchanged from wild-type, the 1.2-nm red-shift of the Soret peak (Figure 3) is likely due to alteration of the environment of heme *a*, and not heme a_3. The FTIR spectrum of the CO-bound enzyme and the EPR spectrum of the oxidized enzyme (not shown) are also identical to those of wild-type. The optical red-shift, therefore, indicates that it is the excited state of heme *a* that is uniquely affected by the alteration of this tyrosine.

DISCUSSION

Interaction of the IX–X Interhelical Loop with Heme a. Callahan and Babcock (1983) showed that the absorption spectra of both reduced and oxidized heme *a* of cytochrome *c* oxidase are red-shifted compared to low-spin model compounds prepared with heme A in solution. They concluded that this shift results from a hydrogen bond between the formyl group of heme *a* and an unidentified amino acid side chain. Indeed, the stretching vibrations of the formyl group, hydrogen-bonded to the protein or hydrogen-bonded to water, have been identified in RR spectra of cytochrome oxidase and heme *a* models (Callahan & Babcock, 1983). The assignment of the 1610-cm^{-1} mode as the hydrogen-bonded formyl group of heme *a* has strong experimental support [but see Ching et al. (1985)]. A hypothetical model of the active site structure of cytochrome oxidase by Saraste (1990) places Tyr-414 of subunit I near the top of helix X and assigns this residue as the hydrogen donor to the heme *a* formyl substituent. Such an arrangement is also possible in more recent models (Hosler et al., 1993; Brown et al., 1993). This would lead to the prediction that conversion of Tyr-414 to phenylalanine, eliminating the capability of this residue to participate in a hydrogen bond, should shift the vibrational mode for the formyl substituent of heme *a* from 1610 cm^{-1} to a higher frequency, closer to that observed in aqueous heme A–imidazole models that lack a strong, directed hydrogen bond (Callahan & Babcock, 1983). In fact, the RR spectrum of Y414F shows no changes from wild-type in the stretching frequencies for either the formyl (1610 cm^{-1}) or vinyl (1624 cm^{-1}) groups (Figure 1), indicating that the protein environment surrounding both of these heme *a* substituents is unaltered. It can be concluded that Tyr-414 does not participate in a hydrogen bond with the heme *a* formyl group.

The question of which residue, if any, might function as the hydrogen donor for this bond remains unanswered. The RR spectra of mutant oxidases with alterations of His-411, Asp-412, and Thr-413 all show wild-type formyl and vinyl stretching modes for heme *a*, demonstrating that none of these residues fulfills this role. Tyr-415 is not highly conserved and thus is a poor candidate. One intriguing possibility is that one of the propionate substituents of heme *a* itself, rather than an amino acid side chain, forms a hydrogen bond with the formyl group. Complex hydrogen bond networks stabilize the charge and conformation of the buried propionate groups of the hemes of soluble cytochrome *c* (Timkovich, 1979), cytochrome *c* peroxidase (Finzel et al., 1984), and catalase (Fita & Rossman, 1985). Therefore, it may be possible to disrupt a propionate–formyl hydrogen bond with mutations that destabilize such a hydrogen bond network.

While the RR spectrum is largely unaffected, conversion of Tyr-414 to phenylalanine leads to a marked change in the optical spectrum of heme *a* (Figure 3). However, the 5-nm red-shift of the α-band of the reduced enzyme is opposite to that predicted for the loss of the formyl hydrogen bond, providing further evidence against that particular role for Tyr-414. A change in the visible absorption spectrum without an altered RR spectrum is not contradictory. The latter technique measures differences in the ground state vibrational levels of the hemes, while the optical absorbance spectrum reflects the energy difference between the ground and electronic excited states, in this case the π–π^* transitions of heme *a*. Thus, the altered protein environment of Y414F primarily affects the excited state of heme *a*.

Since the RR analysis indicates that the protein environment of heme *a* of Y414F is not grossly altered (Figure 1), the interaction responsible for the optical red-shift is likely to be specific and localized. We suggest that the conversion of Tyr-414 to phenylalanine may allow closer interaction of the aromatic side chain of this amino acid with the porphyrin ring

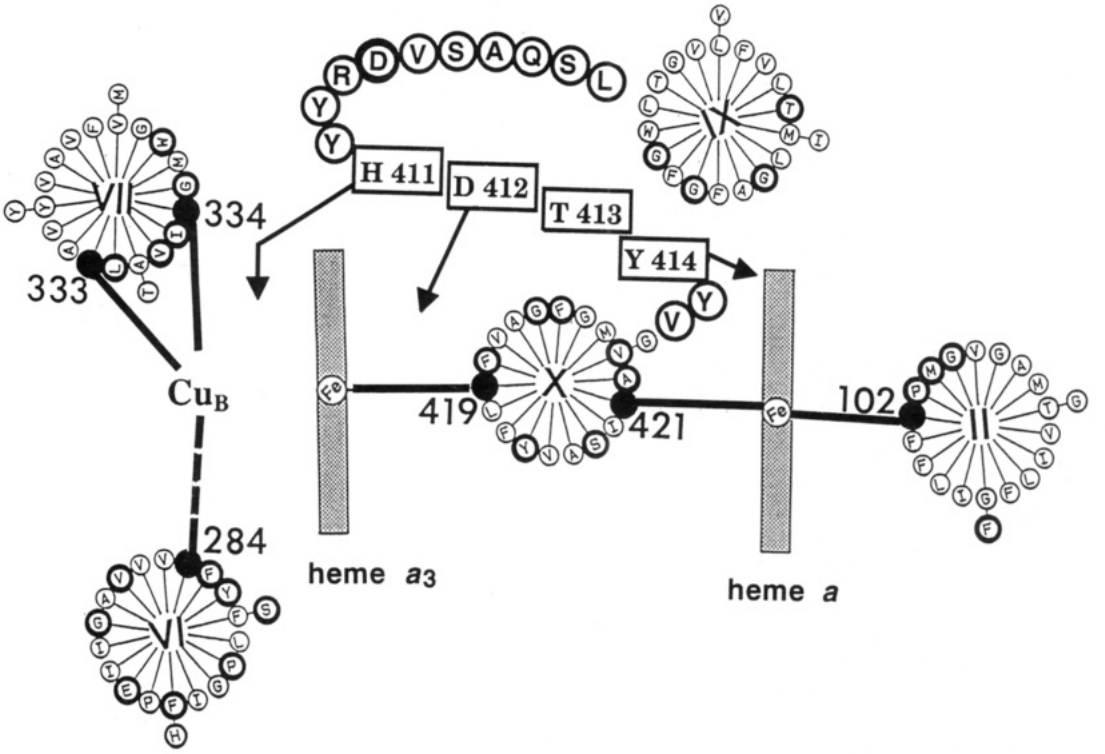

FIGURE 8: Helical wheel model of five of the transmembrane helices of subunit I and the loop between helices IX and X. The histidines that ligate the metal centers of subunit I are darkened and numbered [see Hosler et al. (1993)]. Highly or completely conserved residues, other than the His-411 to Tyr-414 region, are placed within bold circles. The arrows indicate the proposed interactions of His-411 with heme a_3–Cu_B, Asp-412 with heme a_3, and Tyr-414 with heme a.

of heme a. Recent analysis of site-directed mutations affecting the photosynthetic light harvesting complexes of *Rb. sphaeroides* shows that such aromatic interactions are responsible for red-shifts of bacteriochlorophyll a (Fowler et al., 1992).

Our previous analysis of *Rb. sphaeroides* cytochrome aa_3 by EPR spectroscopy suggested the presence of a hydrogen bond of unique strength to one or both of the histidine ligands of heme a (Hosler et al., 1992). Even though this region of the IX–X loop is close to heme a, the fact that none of the mutations alter the g values of the EPR spectrum of eliminates any of these four residues as participants in a hydrogen bond to His-102 or His-421.

The Y414F mutant of *Rb. sphaeroides* cytochrome aa_3 suggests an explanation for the red-shifted α-band (617 nm) of the aa_3-type cytochrome c oxidase of *Tetrahymena pyriformis* (Kilpatrick & Erecinska, 1979). The DNA-derived amino acid sequence of subunit I of the *Tetrahymena* oxidase (Ziaie and Suyama, 1987) indicates that phenylalanine is present at the position equivalent to Tyr-414.

Interactions of the IX–X Interhelical Loop with Heme a_3 and Cu_B. The introduction of asparagine at position 411 severely disrupts the protein environment of heme a_3 and Cu_B and inactivates the enzyme. Indeed, the optical, RR, and FTIR spectra of H411N are similar to those of mutant oxidases in which the histidines that ligate heme a_3 or Cu_B have been altered (Hosler et al., 1993; Shapleigh et al., 1992a). However, the near wild-type spectroscopic characteristics and the significant activity of the alanine mutant at the same position demonstrate that His-411 is not a redox metal ligand (Shapleigh et al., 1992a). In work to be presented elsewhere [see Hosler et al. (1993)] we provide evidence that His-411 and Asp-412 function as ligands of a nonredox active metal, Mn^{2+} (and possibly Mg^{2+}). Since metal binding is lost when His-411 is altered, the replacement amino acid side chains may be free to interact more directly with the heme a_3–Cu_B pocket. In that case, the larger and more polar amide group would be more disruptive than the methyl function supplied by alanine.

While the substitution of alanine for histidine at position 411 is relatively benign, in terms of changes in enzymatic activity and in the optical, RR, and EPR spectra, the alteration in the Cu–C≡O signals in the FTIR difference spectrum (Figure 5) indicates a change in the environment of Cu_B. The apparently stronger α C≡O bond could result from the loss of a hydrogen bond to the copper-bound CO or a ligand rearrangement around Cu_B that increases the electron density on the metal, weakening the Cu_B–C bond and strengthening the C≡O bond.

Substitution of asparagine for aspartate at position 412 of the IX–X loop is considerably less detrimental than the introduction of asparagine at position 411 but appears specific for the environment of heme a_3. Mutant oxidase D412N retains >40% activity (Table 1) and is spectroscopically similar to wild-type, except for a shift in the resonance Raman frequency of the $Fe–N_{His}$ stretch of heme a_3, from 214 to $\sim$218 cm^{-1} (Figure 2). This indicates a slight strengthening of this bond compared to wild-type. The shift in wavenumbers is similar to that observed between the T and R states of hemoglobin (Rousseau & Friedman, 1988) and between the unliganded and recently photolyzed CO-bound forms of heme a_3 of cytochrome oxidase (Findsen et al., 1987). In both of these cases the differences in the frequency of the $Fe–N_{His}$ vibration could result from a small tilt of the proximal histidine in relation to the heme plane (Rousseau & Friedman, 1988; Findsen, 1987) or, alternatively, from increased hydrogen bonding to the backside nitrogen of the imidazole ring of the proximal histidine. A carboxylate group has been postulated to be the hydrogen bond acceptor for the N_δ proton of the proximal histidine of heme a_3 in a recently proposed proton pumping scheme (Rousseau et al., 1993). Our results show

that Asp-412 is unlikely to play this role, since loss of this hydrogen bond would be expected to decrease, rather than increase, the frequency of the Fe–N_{His} stretch (Smulevich et al., 1988). In addition, D412N is capable of proton translocation (Fetter et al., 1993).

The 2-cm^{-1} shift in the α-form of the Fe–C≡O signal (Figure 7) could also result from a small change in the geometry or increased basicity of the proximal ligand. The fact that the extent of CO binding is largely unaffected supports the conclusion that the structural change caused by D412N is on the proximal, rather than the distal, side of heme a_3.

Evolutionary and Functional Considerations. The His-411, Asp-412, Thr-413, Tyr-414 sequence is highly conserved throughout mitochondrial oxidases and the bacterial superfamily of oxidases. From an alignment of 75 subunit I gene sequences (Calhoun, 1993), His-411 is almost completely conserved [substituted by glutamine and serine in two of the three subunit I genes sequences found in *Bradyrhizobium* (Gabel & Maier, 1990; Bott et al., 1990; Preisig et al., 1993)]; Asp-412 is very highly conserved, except in bacterial quinol oxidases, where it is altered to asparagine; Thr-413 is replaced by serine in four sequences; and Tyr-414 is sometimes replaced by phenylalanine (as in *Tetrahymena*). The data presented in this paper suggest that this conserved portion of the connection between putative transmembrane helices IX and X is in contact with both heme *a* and the heme a_3–Cu_B center. This is consistent with the current model that places all three redox active metals near the periplasmic side of the membrane and places the two hemes on opposite faces of helix X (Hosler et al., 1993; Brown et al., 1993). The His-411/Asp-412/Thr-413/Tyr-414 region can be pictured as a cap over the three metal binding sites, with Tyr-414 close to heme *a*, Asp-412 proximal to heme a_3, and His411 distal to heme a_3 and close to Cu_B (Figure 8). Evidence for the importance of this region and its proximity to the metal centers of subunit I also comes from mutational analysis of mitochondrial cytochrome oxidase. The equivalent of D412N in yeast results in the loss of oxidase (Meunier et al., 1993a). Active oxidase is restored, however, by secondary mutations of residues that flank the histidine ligands of Cu_B in transmembrane helix VII (Meunier et al., 1993b; Hosler et al., 1993).

The large hydrophilic domain of subunit II that contains Cu_A is also located on the periplasmic side (outside) of the membrane. Since the distance between Cu_A and heme *a* is estimated to be small (<13 Å; Goodman & Leigh, 1985), this portion of subunit II must be positioned close to the redox active metals of subunit I, and the His-411/Asp-412/Thr-413/Tyr-414 region of the IX–X interhelical loop could be involved in this interaction. The loss of EPR-detectable Mn^{2+} in mutants of His-411 and Asp-412 also suggests the presence of a nonredox active metal in this region (Hosler et al., 1992; and unpublished data), which could play a structural role in the interaction between subunits I and II. Studies on the ligation and significance of this metal center will be reported elsewhere.

In summary, the region of subunit I between His-411 and Tyr-414 appears to be part of a cap over both the heme *a* and the heme a_3–Cu_B centers, supporting the model (Hosler et al., 1993; Calhoun et al., 1993) in which heme *a* and a_3 are both ligated by residues in helix X near the periplasmic side of the membrane.

ACKNOWLEDGMENT

We thank Ms. Kelly Zaslona for expert assistance in oxidase purification and figure preparation, Mr. Einhardt Schmidt for assistance in preparing the RR figures, and Dr. M. Degli Esposti for valuable comments.

REFERENCES

Alben, J. O., & Fiamingo, F. G. (1984) in *Optical Techniques in Biological Research* (Rousseau, D. L., Ed.) pp 133–179, Academic Press, New York.

Babcock, G. T. (1988) in *Biological Applications of Raman Spectroscopy* (Spiro, T.G., Ed.) pp 293–346, Wiley, New York.

Babcock, G. T., Ondrias, M. R., Gobeli, J., Vansteelandt, J., & Leroi, G. E. (1979) *FEBS Lett. 108*, 147–151.

Berry, E. A., & Trumpower, B. L. (1987) *Anal. Biochem. 161*, 1–15.

Bott, M., Bolliger, M., & Hennecke, H. (1990) *Mol. Microbiol. 4*, 2147–2157.

Brown, S., Moody, J., Mitchell, R., & Rich, P. R. (1993) *FEBS Lett. 316*, 216–223.

Calhoun, M. W. (1993) Ph.D. Dissertation, University of Illinois at Urbana-Champaign.

Calhoun, M. W., Thomas, J. W., Hill, J. J., Hosler, J. P., Shapleigh, J. P., Tecklenburg, M. M. J., Ferguson-Miller, S., Babcock, G. T., Alben, J. O., & Gennis, R. B. (1993) *Biochemistry 32*, 10905–10911.

Cao, J., Shapleigh, J., Gennis, R., Revzin, A., & Ferguson-Miller, S. (1991) *Gene 101*, 133–137.

Cao, J., Hosler, J., Shapleigh, J., Revzin, A., & Ferguson-Miller, S. (1992) *J. Biol. Chem 267*, 24273–24278.

Callahan, P. M., & Babcock, G. T. (1983) *Biochemistry 22*, 452–461.

Ching, Y., Argade, P. V., & Rousseau, D. L. (1985) *Biochemistry 24*, 4938–4946.

Fetter, J., Hosler, J. P., Shapleigh. J. P., Thomas, J. W., Tecklenburg, M. M. J., Kim, Y., Gennis, R. B., Babcock, G. T., & Ferguson-Miller, S. (1993) *Biophys. J. 64*, A103.

Fiamingo, F. G., Altschuld, R. A., Moh, P. P., & Alben, J. O. (1982) *J. Biol. Chem. 257*, 1639–1650.

Fiamingo, F. G., Altschuld, R. A., & Alben, J. O. (1986) *J. Biol. Chem. 261*, 12976–12987.

Findsen, E. W., Centeno, J., Babcock, G. T., & Ondrias, M. R. (1987) *J. Am. Chem. Soc. 109*, 5367–5372.

Finzel, B. C., Poulos, T. L., & Kraut, J. (1984) *J. Biol. Chem. 259*, 13027–13036.

Fita, I., & Rossmann, M. G. (1985) *J. Mol. Biol. 185*, 21–37.

Fowler, G. J. S., Visschers, R. W., Grief, G. G., van Grondelle, R., & Hunter, C. N. (1992) *Nature 355*, 848–850.

Gabel, C., & Maier, R. J. (1990) *Nucleic Acids Res. 18*, 6143.

Goodman, G., & Leigh, J. S. (1985) *Biochemistry 24*, 2310–2317.

Hill, B. C. (1991) *J. Biol. Chem. 266*, 2219–2296.

Hosler, J. P., Fetter, J., Tecklenburg, M. M. J., Espe, M., Lerma, C., & Ferguson-Miller, S. (1992) *J. Biol. Chem. 267*, 24262–24272.

Hosler, J. P., Ferguson-Miller, S., Calhoun, M. W., Thomas, J. W., Hill, J., Lemieux, L., Ma, J., Georgiou, C., Fetter, J., Shapleigh, J. P., Tecklenburg, M. M. J., Babcock, G. T., & Gennis, R. B. (1993) *J. Bioenerg. Biomembr. 25*, 121–136.

Janin, J., Miller, S., & Chothia, C. (1988) *J. Mol. Biol. 204*, 155–164.

Kilpatrick, L., & Erecinska, M. (1979) *Arch. Biochem. Biophys. 197*, 1–9.

Kyte, J., & Doolittle, R. F. (1982) *J. Mol. Biol. 157*, 105–132.

Lemieux, L. J., Calhoun, M. W., Thomas, J. W., Ingledew, J., & Gennis, R. B. (1992) *J. Biol. Chem. 267*, 2105–2113.

Meunier, B., Lemarre, P., & Colson, A.-M. (1993a) *Eur. J. Biochem. 213*, 129–135.

Meunier, B., Coster, F., Lemarre, P., & Colson, A.-M. (1993b) *FEBS Lett. 321*, 159–162.

Minagawa, J., Mogi, T., Gennis, R. B., & Anraku, Y. (1992) *J. Biol. Chem. 267*, 2096–2104.

Preisig, O., Anthamatten, D., & Hennecke, H. (1993) *Proc. Natl. Acad. Sci. U.S.A. 90*, 3309–3313.
Rousseau, D. L., & Friedman, J. M. (1988) in *Biological Applications of Raman Spectroscopy* (Spiro, T. G., Ed.) pp 133–215, Wiley, New York.
Rousseau, D. L., Ching, Y.-c., & Wang, J. (1993) *J. Bioenerg. Biomembr. 25*, 165–175.
Saraste, M. (1990) *Q. Rev. Biophys. 23*, 331–366.
Shapleigh, J. P., & Gennis, R. B. (1992) *Mol. Microbiol. 6*, 635–642.
Shapleigh, J. P., Hosler, J. P., Tecklenburg, M. M. J., Kim, Y., Babcock, G. T., Gennis, R. B., & Ferguson-Miller, S. (1992a) *Proc. Natl. Acad. Sci. U.S.A. 89*, 4786–4790.
Shapleigh, J. P., Hill, J. J., Alben, J. O., & Gennis, R. B. (1992b) *J. Bacteriol. 174*, 2338–2343.
Smulevich, G., Mauro, J. M., Fishel, L. A., English, A. M., Kraut, J., & Spiro, T. G. (1988) *Biochemistry 27*, 5477–5485.
Timkovich, R. (1979) in *The Porphyrins* (Dolphin, D., Ed.) Vol. VII, pp 241–294, Academic Press, New York.
Vanneste, W. H. (1966) *Biochemistry 5*, 838–848.
Yoshikawa, S., & Caughey, W. S. (1982) *J. Biol. Chem. 257*, 412–420.
Zamyatnin, A. A. (1972) *Prog. Biophys. Mol. Biol. 24*, 107–123.
Ziaie, Z., & Suyama, Y. (1987) *Curr. Genet. 12*, 357–368.